Development of true triaxial testing system to evaluate anisotropy of elastic characteristics on sedimentary soft rock

Développement d'un essais véritablement triaxial afin d'évaluer l'anisotropie des roches tendres sédimentaires dans le domaine des déformations élastiques

K.Hayano & T.Sato – *Institute of Industrial Science, University of Tokyo, Tokyo, Japan*

ABSTRACT: A new high-precision true triaxial testing apparatus with local strain measurement was developed to accurately evaluate the stress-induced anisotropy of Young's modulus at small strains on sedimentary soft rock. This stress-induced anisotropy on Young's modulus could be rationally explained by the following assumption as the E_z is basically a function of the σ'_z and the E_y is a function of the σ'_y respectively.

RÉSUMÉ: A nouvelle machine de compression triaxiale vrai, a haute precision avec mesure des deformations locales a ete developpee au fin de calculer l' anisotropie induite du module de Young, a petits niveaux de deformation sur une roche souple sedimentaire. Cette anisotropie induite du module de Young pourrait etre logiquement expliquee en faisant l' assomption que E_z est essentiellement une fonction de σ'_z et que E_y est une fonction de σ'_y, respectivement.

1 INTRODUCTION

Recently the numbers of long-suspension bridges, liquid natural gas tanks and dams constructed on sedimentary soft rocks have been increased (Tatsuoka and Kohata, 1995). Sedimentary soft rock deposits are also often excavated for the tunnels and stations of subways (Miyazaki et al., 1999). In those constructions, the deformation caused by the working loads of the foundations or excavations should be strictly sustained related to the stability of the structure and the environmental risks. As the elastic behaviour domains in the deformation of relatively stiff geomaterials, accurate evaluation of elastic modulus should be important. Related to the above, a number of attempts have been made to evaluate the deformation characteristics of sedimentary soft rocks by triaxial compression tests measuring axial strain locally (e.g., Jardine et al. 1985, Kim et al. 1994).

However, the stress-induced anisotropy of elastic deformation on sedimentary soft rocks has been investigated only to a limited depth. In view of the above, a new high-precision true triaxial testing apparatus with local strain measurement was developed. To accurately evaluate the stress-induced anisotropy of Young's modulus at small strains, two series of very small cyclic axial and lateral loading tests were performed on a rectangular specimen of sedimentary soft mudstone. In this paper, the characteristic features of the new testing system including an important technical problem and some typical results on the sedimentary soft mudstone will be presented.

2 TRUE TRIAXIAL TESTING SYSTEM

The newly developed true triaxial testing system is shown in Figs. 1 and 2. This system consists of a triaxial cell having a capacity of 3MPa, a local measurement system for vertical and horizontal strains, a new lateral loading systems, a cell pressure system, a high-precision hydraulic axial loading system and a data acquisition system. The confining pressure σ'_x, the lateral load F_y and the vertical strain ε_z can be controlled independently.

The structure of the lateral loading system as shown in Fig. 2 is similar to that developed for the plane strain compression apparatus for soft rocks (Hayano et al., 1999). Three miniature oil cylinders (OCs) are fixed with bolts between the stainless steel confining platen (CFP1) and the end plate (EP1). The cylinders have a capacity of 15kN for the lateral load F_y. The value of F_y is

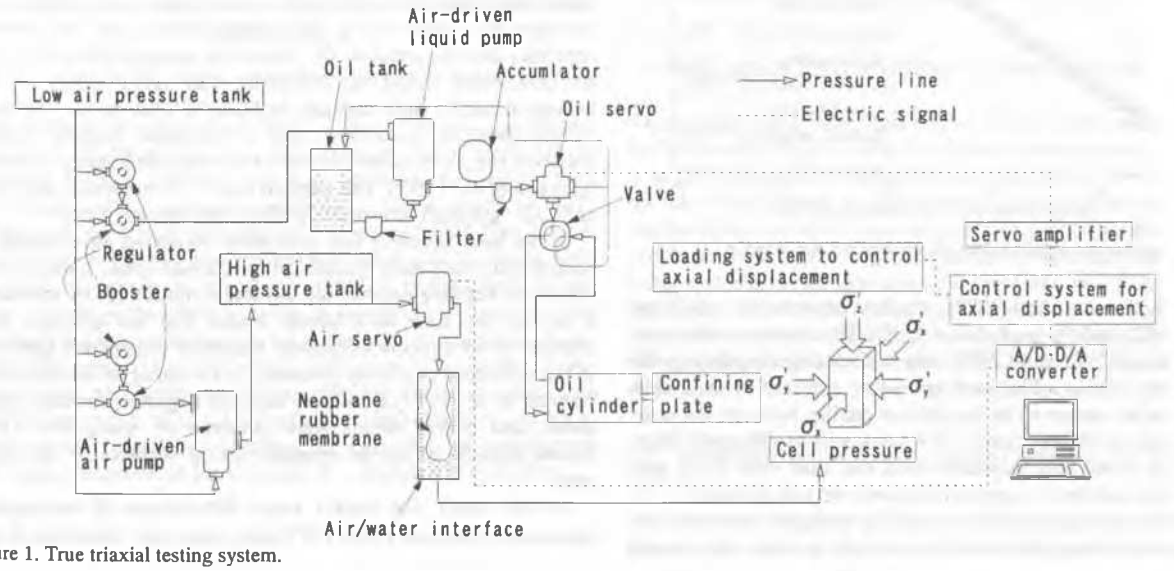

Figure 1. True triaxial testing system.

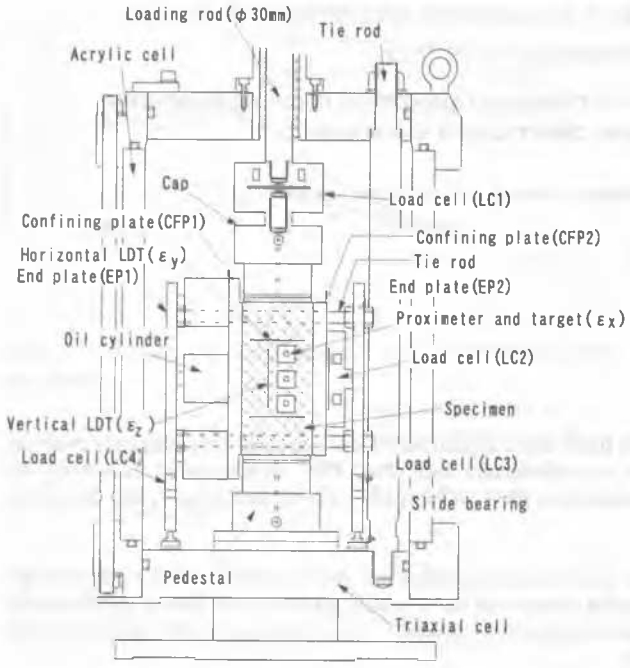

Figure 2. Triaxial cell with lateral loading system.

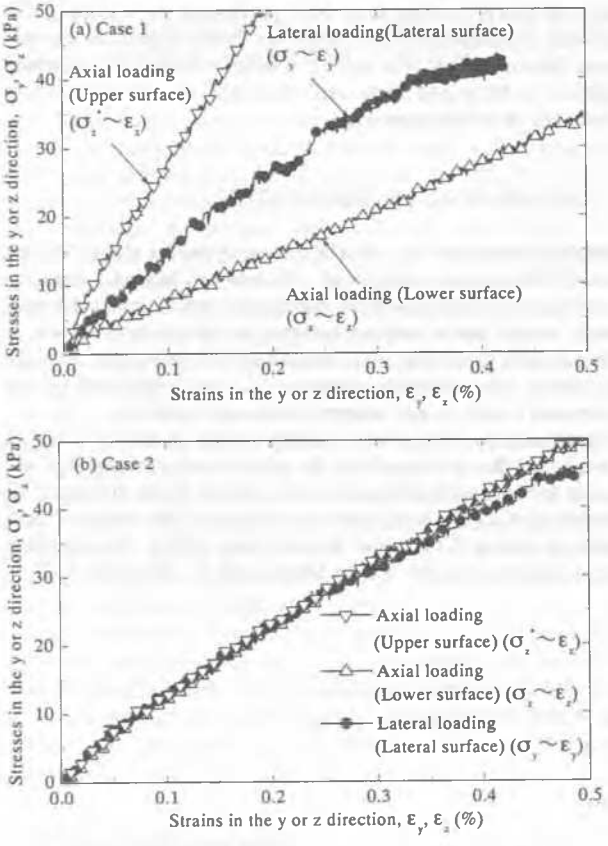

Figure 3. Stress-strain relationships on the dummy specimen.

measured with a load cell (LC2), attached between the confining platen (CFP2) and the end platen (EP2). The stainless steel confining platens (CFP1 and CFP2) have well-polished surfaces with a minimum friction. The surfaces were smeared with a thin grease layer to improve the lubrication quality between the confining plates and the specimen. This point will be discussed later. The friction force was measured with two load cells (LC3 and LC4) during each test to correct measured vertical stresses.

A pair of end platens (EP1 and EP2) is tightly connected to each other by using four stainless tie-rods to make the lateral

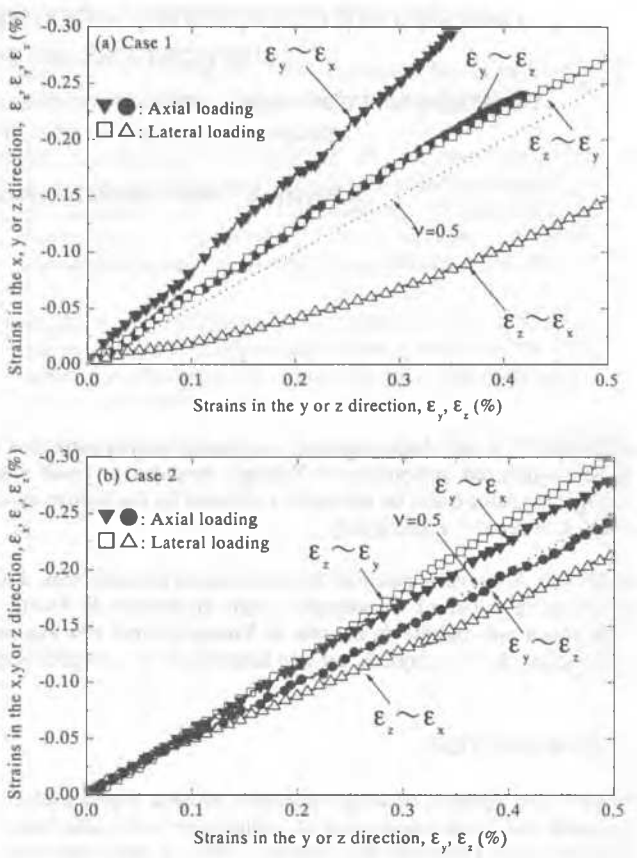

Figure 4. Strain-strain relationships on the dummy specimen.

loading system rigid enough. Due to inevitable imperfectness of setup, if the end platens were rigidly fixed to the triaxial cell, large unwanted load would be exerted to the test system and the specimen as the specimen deforms. Therefore, for smooth lateral displacement of the confining platens, the end platens (EP1 and EP2) are supported with four small slide tables having ball bearings placed on the base of the triaxial cell.

The lateral loading system, to control the lateral load F_y independently of the other two principal stresses, consists of three miniature oil cylinders (OCs), an air-driven oil pump, an accumulator (to reduce fluctuations in pressure) and an oil-servo. The pump can amplify original oil pressure by a factor of 25, up to about 15MPa, through a servo-amplifier. The oil-servo controls the oil pressure supplied to the oil cylinders based on analog signals from the D/A board. The confining pressure control system consists of an air-driven air pump and an air-servo (i.e., an electronic-pneumatic transducer). The pump can amplify original air pressure by a factor of 6, up to about 3MPa, and an air-servo regulates the cell pressure σ'_x based on analog signals from a 12 bit D/A board inside the computer. The cell pressure σ'_x is measured with a high-capacity differential transducer. The axial displacement is controlled with a hydraulic loading system, which is free from backlash when reversing the loading direction (Hayano et al., 1997). The vertical load F_z is measured with load cell LC1, attached immediately above the specimen cap.

It has been revealed that externally measured axial strains of sedimentary soft rock cylindrical specimens could include large effects of bedding error at the top and bottom ends of specimen. It is also the case with lateral strains that are obtained from changes in the specimen diameter measured outside the specimen if the effective confining pressure is changing in triaxial tests. Hayano et al., 1997, therefore, used rectangular-prismatic specimens, and lateral strains were obtained by using four LDTs placed laterally along the opposite lateral surfaces of the specimen.

In this study, the nearly same dimensions of rectangular specimen as Hayano et al., 1997 were employed, which are 6 cm-

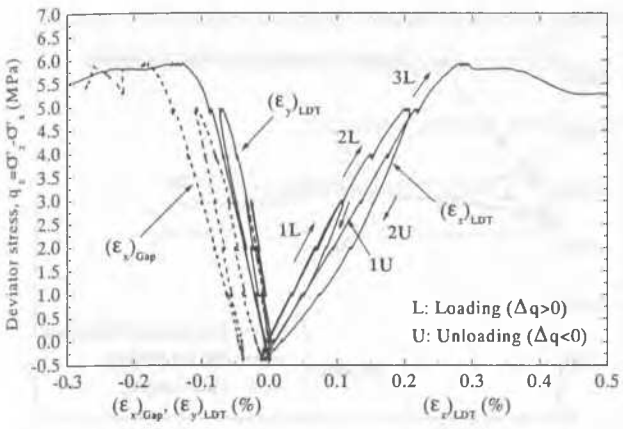

Figure 5. The relationships between the deviator stress $q_z=\sigma'_z-\sigma'_x$ and the strains ε_z, ε_x, ε_y.

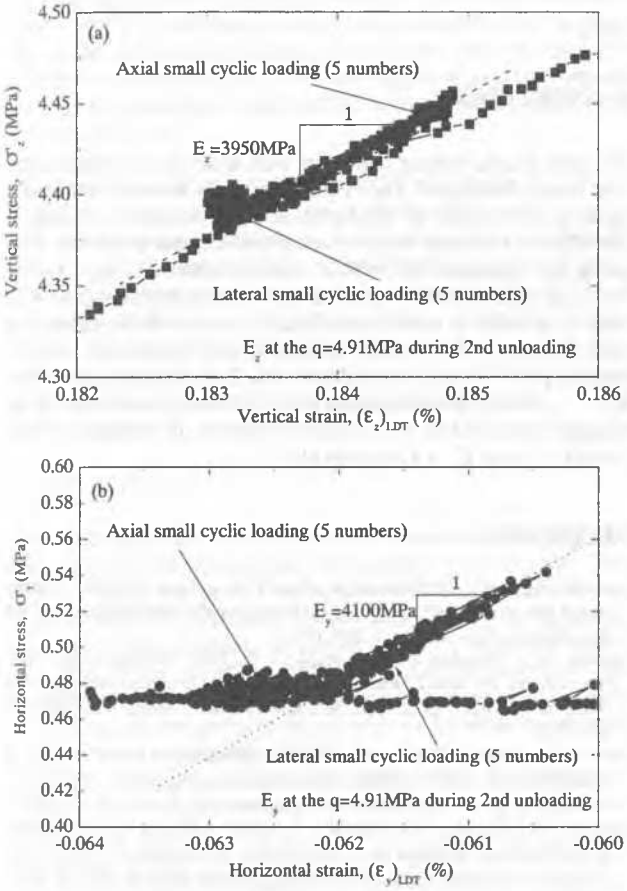

Figure 6. Stress–strain relationships from typical cyclic tests.

wide in the x-direction, 8 cm-long in the y-direction and 16 cm-high in z-direction (Fig. 2). The three principal strains were measured locally. Strains ε_z and ε_y in the z- and y-directions were measured by using, respectively, a pair of vertical LDTs (Goto et al., 1991) and two pairs of horizontal LDTs. The LDT is a clip gauge made of a phosphor bronze strip, which detects, with electrical resistance strain gauges attached at the center of the strip, changes in the distance between the two ends fixed to a pair of targets (hinges) attached on the surface of the specimen membrane. The vertical and horizontal LDTs used in the present study had a length of 70 mm and 60 mm, respectively, with a thickness of 0.25 mm and a width of 0.2 cm. The other strain ε_x in the x-direction was measured by using the two pairs of proximeters and targets attached on the opposite σ'_x surfaces of specimen.

2.1 *The effects of frictions on the boundaries*

Since the rigid platen constrains the deformation of the specimen, the friction force on the boundaries between the specimen and the rigid platens was considered as an important technical problem. Therefore, preliminary tests were conducted on the dummy specimen, which was subjected to monotonic axial and lateral loading independently to evaluate the effects of friction force on the deformation characteristics. The neoprene rubber was used as the rectangular dummy specimen. The specimen was set in the apparatus with the following manners;

Case 1: The specimen was directly contacted with the confining platens, cap and pedestal.

Case 2: Lubrication layers were prepared between the specimen and all rigid platens (the cap, the pedestal and the confining plates)

Fig. 3 shows the stress-strain relationships when the axial and lateral monotonic loadings were applied to the specimen in each condition. Fig. 4 shows the strain-strain relationships, which are the $\varepsilon_z \sim \varepsilon_x$, $\varepsilon_z \sim \varepsilon_y$ relationships in the vertical loading and the $\varepsilon_y \sim \varepsilon_x$, $\varepsilon_y \sim \varepsilon_z$ relationships in the lateral loading. In these tests, the confining pressure σ'_x was kept zero. The vertical stress σ'_z was obtained from the value of F_z measured with the load cell (LC1) shown in Fig. 1. The σ_z was the corrected vertical stress by taking account the frictional force measured with the two load cells (LC3 and LC4) into the value of F_z. The horizontal stress σ_y was obtained from the value of F_y measured with the load cell (LC2). In the lateral monotonic loading, the value of F_z was controlled to keep the value of σ_z constant. In the vertical loading, the value of F_y was controlled to keep the σ_y constant.

In the tested condition "case 2", the stress-strain relationship ($\sigma_y \sim \varepsilon_y$) obtained from the lateral loading shows the same behaviour as those ($\sigma'_z \sim \varepsilon_z$ and $\sigma_z \sim \varepsilon_z$) obtained from the axial loading as shown in Fig.3(b). In this condition, the Poisson's ratios ν, which were nearly equal to 0.5 were also obtained as shown in Fig. 4(b). On the other hand, in the tested condition "case 1", the stress-strain relationships obtained from the axial and lateral loadings, showed the different behaviour as shown in Fig. 3(a). The Poisson's ratios ν were also obtained, but they were quite scattered (Fig. 4(a)). Therefore, the test results obtained from "case 1" cannot explain the deformation characteristics of neoprene rubber specimen, which was considered basically as the isotropic material.

In "case 2", the friction force was nearly equal to zero along confining plates, as the values of σ'_z and σ_z were nearly same. However, in "case 1", the differences between the σ'_z and the σ_z were quite large. Therefore, it was concluded that the lubrication layers are essential between the specimen and all rigid platens to evaluate the anisotropy of deformation characteristics accurately from axial and lateral loadings.

3 TEST RESULTS ON SEDIMENTARY SOFT MUDSTONE

The samples that were used in the present study were retrieved by block sampling at a depth of about 50 m from a 1.5 million year old sedimentary soft mudstone deposit at the Sagamihara test site. The deposit is well-cemented, and nearly unweathered and continuous with a mean diameter D_{50} equal to about 0.006 - 0.02 mm. Rectangular prismatic samples were manually trimmed using a cutter in the laboratory. A specimen was fully saturated by means of the vacuum method, followed by back-pressurizing to 196kPa in a triaxial cell filled with de-aired water. To facilitate the drainage of specimen, a side drain of filter paper, connected to the side drain of the cap and pedestal, was used.

3.1 *Testing method and stress induced anisotropy of Young's modulus*

The specimen was first compressed isotropically from 30 to 1600 kPa, during which and at the different isotropic stress states, a se-

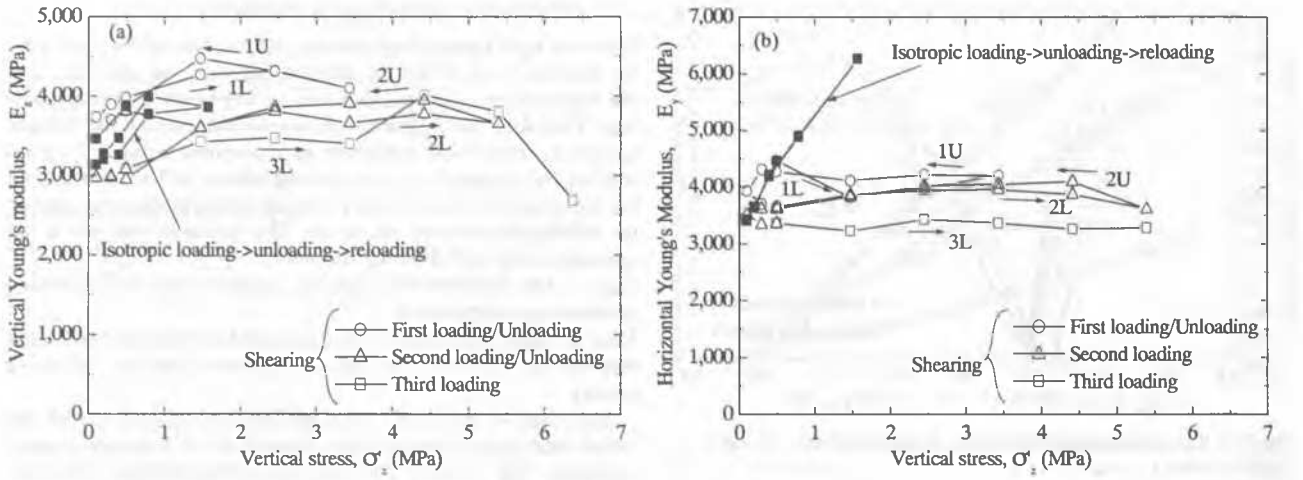

Figure. 7 Young's modulus at the isotropic and drained shearing states((a) E_z, (b)E_y).

ries of very small cyclic axial and lateral loading tests were performed under drained conditions. Then the specimen was isotropically rebounded from 1600 to 470 kPa and sheared with keeping the horizontal stresses σ'_x and σ'_y basically constant. For shearing, a few numbers of large-amplitude cyclic loading were applied under drained conditions and finally the specimen was brought to failure (Fig. 5). During these large-amplitude cycles, a series of very small cyclic axial and lateral loading tests were also performed under drained conditions at the different levels of $q_z = \sigma'_z - \sigma'_x$ under isotropic or anisotropic stress conditions. The vertical strain rate was constant throughout these tests, that was 0.002 %/min.

To investigate into the stress state-dependency of small strain deformation properties, the vertical and horizontal Young's moduli E_z and E_y of the specimens were evaluated by applying the following a series of very small cycles of axial and lateral stresses at various stress levels during isotropic loading and shearing: 1) Axial small cyclic loading; Keeping constant the stresses σ'_x and σ'_y in the x and y directions, stress increments $d\sigma'_z$ in the z direction were applied five times by controlling the axial displacement. 2) Lateral small cyclic loading; Keeping constant the stresses σ'_x and σ'_z in the x and z directions, stress increments $d\sigma'_y$ in the y direction were applied five times by controlling the F_y.

The stress σ'_y in the former tests and the stress σ'_z in the latter tests were kept constant by using a computer-aided feedback system based on outputs from load cells LC2 and LC1, respectively.

Figs. 6 a) and b) show stress–strain relationships from typical cyclic tests. The stress-strain behaviour is nearly perfectly linear and reversible with a negligible hysteresis. Yet, as the behaviour is not perfectly elastic, these properties will herein be called quasi-elasticity. The vertical and horizontal quasi-elastic Young's moduli E_z and E_y were evaluated from the average slopes of such relationships between σ'_z and ε_z and between σ'_y and ε_y. Fig. 7 shows the relationships between the E_z, E_y values and the stress levels, which were represented by the σ'_z ($=\sigma'_y$) values during the isotropic compression and the σ'_z values during the drained shearing. Fig. 7 shows that the E_z and E_y values at the isotropic stress states increases with the stress level, $\sigma'_z = \sigma'_y$. It is seen that during the drained shearing, the E_z value increases as σ'_z increases, while the E_y value remains basically constant. It is seen by detailed explanation of the test that by the effect of the large cyclic loading, the E_z and E_y values gradually decrease when compared at the same stress level. Summarizing the stress-state dependency of E_z and E_y, the effect of σ'_z on E_z was clearly seen, while E_y was not affected by σ'_z. These trends could be rationally explained by the assumption that E_z is basically a function of σ'_z and E_y is a function of σ'_y.

4 CONCLUSION

The true triaxial testing apparatus with local strain measurement was newly developed. The lubrication layers between the rectangular specimen and all rigid platens were essential to minimize the effects of friction forces on deformation characteristics. With using the apparatus, the vertical and horizontal Young's moduli E_z, E_y at small strains of sedimentary soft mudstone were evaluated by a series of small cyclic loading tests in the axial and lateral directions. The results indicated such stress-state induced anisotropy of Young's modulus as that E_z is uniquely controlled by σ'_z while E_y is independent of σ'_z. These trends could be rationally explained by the assumption that E_z is basically a function of σ'_z and E_y is a function of σ'_y.

REFERENCES

Goto, S., Tatsuoka, F., Shibuya, S., Kim, Y. S. & Sato, T. 1991, *A simple gauge for local small strain measurements in the laboratory*, Soils and Foundations, Vol. 31, No. 1, 169-180.

Jardine, R. J., Brookes, N. J. & Smith, P. R. 1985, *The use of electrical transducers for small strain measurements in triaxial tests on weak rock*, Int. J. Rock. Mech. Min. Sci. and Geomech. Abstr. Vol. 22, No. 5, 331-337.

Hayano, K., Sato, T. & Tatsuoka, F. 1997, *Deformation characteristics of a sedimentary soft mudstone from triaxial compression tests using rectangular prism specimens*, Geotechnique, Vol. 3, No. 47, 439-450.

Hayano, K., Maeshiro, T., Tatsuoka, F., Sato, T., Wang, L. and Kodaka, T. 1999, *Shear banding in a sedimentary soft mudstone subjected to plane strain compression*, Geotechnical Testing Journal, Vol. 22, No.1, 67-79.

Kim, Y. S., Tatsuoka, F. & Ochi, K. 1994, *Deformation characteristics at small strains of sedimentary soft rocks by triaxial compression test*, Geotechnique, Vol. 44, No. 3, 461-478.

Miyazaki, K., Hayano, K., Tatsuoka, F. & Koseki, J. 1999, *Deformation of sedimentary soft rock in deep excavation*, In Pre-failure deformation of geomaterials (Jamiolkowski et al. eds.), Balkema, Vol. 1, 809-818.

Tatsuoka, F. & Kohata, Y. 1995, *Stiffness of hard soils and soft rocks in engineering applications*, In Pre-failure deformation of geomaterials (Shibuya et al. eds.), Balkema, Vol. 2, 947-1063.